Healing kinetics of microneedle-formed pores in PLGA films

J.M. Mazzara [a,c], M.A. Balagna [a,c,d], M.D. Thouless [b,d], S.P. Schwendeman [a,c,*]

[a] Department of Pharmaceutical Sciences, University of Michigan, 428 Church St., Ann Arbor, USA
[b] Department of Mechanical Engineering, University of Michigan, 2350 Hayward St., Ann Arbor 48109, USA
[c] Biointerfaces Institute, University of Michigan, NCRC, 2800 Plymouth Road, Ann Arbor, USA
[d] Department of Materials Science & Engineering, University of Michigan, 2350 Hayward St., Ann Arbor 48109, USA

ARTICLE INFO

ABSTRACT

The spontaneous healing of aqueous pores in poly(D,L-lactic-co-glycolic acid) (PLGA) drug delivery systems has been identified to play a key role in terminating the burst release of large molecules, and to provide a means for novel aqueous-based microencapsulation. To examine healing of PLGA, pores were created of defined size and depth on the surface of thin PLGA films by stamping with blunt-tip microneedles. Pore dimensions on the micron-scale were relevant to surface pores of common PLGA microspheres and could be easily monitored by light microscopy. Most pores healed reproducibly at temperatures above the glass-transition temperature (T_g) of the films, with healing times decreasing sharply with increasing temperature according to Williams–Landel–Ferry (WLF) behavior. It is suggested that healing is driven by high surface tension in the films and occurs through viscoelastic creep. Hydrated films healed at lower temperatures than dry films, consistent with a drop in T_g upon polymer hydration. Larger pores took longer to heal than smaller ones, while pores larger than 20 μm did not heal before significant polymer degradation occurred. Films of a less hydrophobic PLGA showed slower healing kinetics, attributed to a weaker surface tension driving force. Deeper pores showed signs of in-plane stress from spin-coating, and either ruptured or only partially healed when incubated wet and dry, respectively.

© 2013 Published by Elsevier B.V.

1. Introduction

Poly(D,L-lactic-co-glycolic acids) (PLGAs) have been studied exclusively for controlled release devices for delivery of peptides, proteins, vaccine antigens and even nucleic acids [1–6]. Despite their widespread use over more than four decades, a few fundamental physical–chemical properties of PLGAs having significant impact on their biomaterial performance have nonetheless remained elusive. An important example involves the spontaneous self-healing of pores in the polymer that are created during processing (e.g., microencapsulation and drying) and incubation. This phenomenon has been shown to play an important role in encapsulation and release of drugs and peptides [7–12], and could become of increased significance as the pharmaceutical pipeline becomes increasingly biologic, and greater precision and control is required of long-term controlled release devices.

Passive healing in polymers is a known occurrence [13], and can reasonably be expected to occur and have similar relevance in numerous other biomaterials (e.g., poly(ethylene-co-vinyl) acetate and silicone rubber) commonly used for controlled release. For example, during previous evaluation of the release kinetics of a cyclic peptide, octreotide,

from PLGA microspheres, the pores on the surface of the polymer were observed to slowly heal over a time-scale of hours in an aqueous medium [7]. The sealing of the surface pores was found to correspond to both the cessation of the initial burst release of peptide, and a sharp reduction in effective permeability of fluorescent markers capable of entering the polymer matrix by pore-diffusion [7]. Similar behavior was also observed with bovine serum albumin (BSA) and dextran-loaded PLGA microspheres [14]. As the temperature was raised to a physiological temperature or above (i.e., above T_g of the hydrated polymer [15]), the initial burst release of both dextran and BSA dropped as polymer healing became more rapid. The use of pore-markers incubated outside the PLGA microspheres indicated that the healing of pores also occurred during the degradation phase of the polymer, suggesting a two-way valve mechanism of large molecule release [14]. Finally, spontaneous pore closing in water has recently been shown to facilitate encapsulation of macromolecules [8,9,13] without exposing them to the damaging organic solvents and sterilizing conditions used in traditional methods [16–22].

In order to better understand healing in PLGAs, we sought to develop a system that could be used to reproducibly evaluate the kinetics and mechanism of self-healing in the polymer. To accomplish this, we exploited blunt microneedles, capable of creating well-defined pore morphologies within the surface of PLGA films. The purpose of this paper is to describe this simple development and the key findings related to the kinetic behavior of PLGA self-healing of pores from a variety of pore sizes and depths.

* Corresponding author at: Biointerfaces Institute, University of Michigan, NCRC, 2800 Plymouth Road, Ann Arbor, USA. Fax: +1 734 615 6162.
E-mail address: schwende@umich.edu (S.P. Schwendeman).

2. Materials and methods

2.1. Materials

Unless otherwise specified, the PLGA used was poly(D,L-lactic-co-glycolic acid) 50:50 with lauryl ester-terminated chains, inherent viscosity (i.v.) and weight-averaged molecular weight (Mw) of 0.61 dl/g in hexafluoroisopropanol (HFIP) at 25 °C and 55.3 kDa, respectively (Lactel Inc., Birmingham, AL). PLGA 504H (50:50, carboxylic acid-terminated, $Mw = 38–54$ kDa, $i.v. = 45–60$ dL/g) was purchased from Sigma-Aldrich (St. Louis, MO). All other chemicals were of analytical grade or higher.

2.2. Fabrication of blunt-tip microneedle stamps

The general pattern of the stamps consisted of an array of square needles with inter-needle distance set at $10\times$ needle width. Needles ranged between 1 and 250 µm-wide squares, while the depth was set at 7 or 15 µm. The smaller arrays (≤ 5 µm) were surrounded by a larger square (1 mm thick) so the target area could be easily located. Three separate stamps were used; one with needles 1, 2, 3, and 5 µm wide, 7 µm deep. The second contained needles 10, 20, 30, and 50 µm wide, also 7 µm deep. The final stamp had needles 50, 100, 150, and 250 µm wide, but 15 µm deep.

To form the microneedle stamps, a negative of the design was first drafted in L-edit (Tanner Research, Monrovia, CA), scaled up $5\times$ from the final feature size. This was fractured into a series of squares and rectangles used to shoot the photomask reticle. The pattern was then exposed onto a 127 mm photomask spin-coated with positive photoresist. After exposure, the photomask was developed in developer solution and the exposed areas were etched with chrome etchant before stripping away the remaining photoresist. The mask was then loaded into a stepper (GCA AS 200, Andover, MA), which scaled the feature size down by $5\times$, and the proper exposure times were determined incrementally. Silicon wafers were coated with 2.5 µm of positive photoresist (SPR 220 (3.0) series resist) by an ACS Cluster tool (SUSS MicroTec, Garching, Germany) and then etched (STS Pegasus 4, San Jose, CA) accordingly. The remaining photoresist was then stripped away and the wafers were characterized by contact profiling and SEM. Finally, the wafers were diced (ADT 7100, Horsham, PA) into usable sizes before being glued to a plastic dowel for grip.

2.3. Film preparation and stamping

PLGA films were prepared by dissolving the PLGA in acetone (27% w/w) and then spin-coating the solution onto cover-glass slides using a G3-8 Spin Coater (Specialty Coating Systems Inc., Indianapolis, IN). The volume used was 0.25 mL, coating time was 7 s, and the spin speeds were 1515 and 3200 rpm for ester- and acid-terminated polymers, respectively. The thicknesses of the films were determined by a microcaliper (Marathon, Ontario, Canada). Immediately after spin-coating, the microneedle stamps were gently pressed onto the film surface to create the indentation and then removed. Films were then dried for 24 h in a fume-hood and 24 h under vacuum. Sample quality was ensured by viewing each sample on a light microscope (Axiolab, Carl Zeiss, Oberkochen, Germany) with $5–40\times$ magnification. Images were taken with a Canon Rebel EOS XSi equipped with a $2.5\times$ phototube (Carl Zeiss) attached to the microscope. All samples were imaged prior to incubation for reference. Excess glass and polymer were cut away from the stamp area and the samples were stored at 4 °C until further use.

2.4. Film incubation

For incubation under aqueous conditions, the films were placed in plastic Petri dishes (5 cm diameter) and filled with 7 mL pre-warmed buffer solution before capping and allowed to stand during incubation (Precision, Thermo Scientific, Waltham, MA). The standard buffer was PBS (137 mM NaCl, 2.7 mM KCl, 10.1 mM Na_2HPO_4, 1.7 mM KH_2PO_4) + 0.02% Tween 80, pH 7.4 (PBST). At predetermined times, the media were discarded, and the films were rinsed with distilled and deionized H_2O to prevent salt formation. The films were then patted dry with tissue paper before immediate imaging. Three replicates were used for each time point and the samples were discarded after imaging.

Films incubated without aqueous media were placed and capped in the same Petri dishes under ambient conditions before being placed in the incubator. At predetermined times, they were removed from the incubator, imaged quickly, and then returned for further incubation.

2.5. Thermal analysis

The amount of residual solvent was determined by thermogravimetric analysis (TGA) (Discovery, TA Instruments, New Castle, DE) as previously reported [22]. Briefly, 15–20 mg of sample was placed on platinum pans before equilibrating at 25 °C. The temperature was then ramped to 600 °C at 10 °C/min. The solvent loss was determined from the mass lost between 25 °C and 150 °C, which is much lower than the temperature range over which significant mass loss of the polymer occurs.

Glass-transition temperatures were determined by modulated differential scanning calorimeter (MDSC) (Discovery, TA Instruments, New Castle, DE). Approximately 10 mg of sample were crimped in aluminum pans. Temperatures were ramped between −20 °C and 150 °C (80 °C for hydrated films) at 3 °C/min, with a modulation amplitude of $+/−1$ °C/min (1.5 °C/min for hydrated films) and a period of 60 s. All samples were subjected to a heat/cool/heat cycle. The glass-transition temperatures of hydrated films were determined by soaking them in PBST at room-temperature for 1 h before patting dry, removing the glass substrate and sealing with hermetic lids. The analysis was done using TA TRIOS software, and all experiments were performed in triplicate.

3. Results

3.1. PLGA films with microneedle-stamped pores

Spin-coating under the given conditions produced films 26 ± 3 and 24 ± 4 µm thick (mean $\pm$ SEM, $n = 9$) for ester- and acid-terminated films, respectively. The films began to dry rapidly after coating, so applying the microneedle stamps had to be done immediately. Each film was stamped several times in different locations, and the individual stamps were cut out after drying. Using the 1–5-µm stamp, only the 5-µm needles repeatedly produced usable pores. In some instances, and particularly with larger pores, a ridge appeared around the pores as a result of in-plane compressive stresses. This appears as a black ring in some light microscope images.

After drying, the films appeared generally uniform and transparent with a modest level of roughness (Fig. 1). No significant differences were observed between the two PLGAs used, although different spin-speeds were required to achieve similar thicknesses. Pores ranged between 5 and 250 µm in width. The 5-µm-wide, 7-µm-deep pores were used for all experiments except when the effect of pore size was evaluated, as described below. The levels of residual solvent and glass-transition temperatures are presented in Table 1.

3.1.1. Effect of temperature on healing time in PBST

When PLGA films were incubated in PBST at temperatures of 43 °C and above, the pores slowly healed until the surface became uniform and no evidence of the pores could be observed by light or scanning electron microscopy (SEM). For example, in Fig. 2a films are displayed at different stages of the healing process under aqueous conditions. The morphology of the pores suggests that healing occurs both from
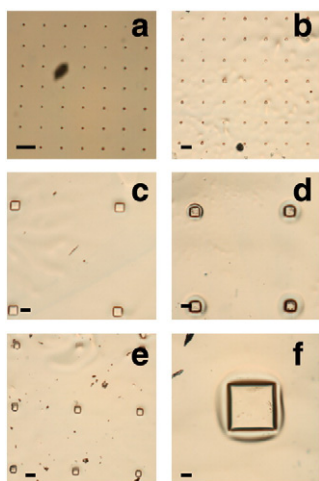
Fig. 1. Representative light micrographs of PLGA films with various surface pores created by blunt-tip microneedle stamps. 7 μm deep and a) 5 μm wide, b) 10 μm wide, c) 50 μm wide, e) 30 μm wide; and 15 μm deep and d) 50 μm wide and f) 250 μm wide. Scale = 50 μm.

Fig. 2. Healing of surface pores in a) PBST and b) air after; 1) 0 h, 2) 2 h, 3) 4 h, 4) 6 h, and 5) 8 h. Scale = 50 μm.

the edges in and from the bottom up, as the initially square pores quickly became circular, but the outline of the pore could be observed throughout healing. The film around the pores became rougher as the incubation continued, likely due to hydration of the film or from buffer solution trapped between the film and the glass substrate after drying. As the incubation temperature increased, the healing times decreased, as shown in Fig. 3a.

When films were incubated at 37 °C, they became an opaque milky-white, and SEM was required to evaluate pore morphology. Here, the early stages of healing could be observed (rounding out of pores and some loss of definition) but full healing did not occur after 2 weeks. Results were similar when incubated at 25 °C for 1 week, although the films remained translucent and any change to pore morphology was minimal. Finally, when incubated at 5 °C the films' morphology did not change, and remained smooth during a 1-week incubation, suggesting only minimal hydration of the glassy polymer (Supplementary information).

3.1.2. Effect of temperature on dry healing

When the films were incubated dry, the required healing times jumped significantly, and the minimal required temperature to observe healing at reasonable time scales rose to 50 °C. Similar to the behavior of wet films, further increases in temperature reduced healing time, as shown in Fig. 3b. The pores also behaved in a similar fashion, becoming less well defined over time. In contrast to the wet films, the parts of the films surrounding the pores remained smooth throughout incubation (Fig. 2b).

3.1.3. Healing kinetics of carboxylic acid-terminated PLGA

When the more hydrophilic carboxylic acid-terminated PLGA 504H was used in healing studies, the rate of healing slowed considerably. When incubated in PBST at 50 °C, healing did not complete
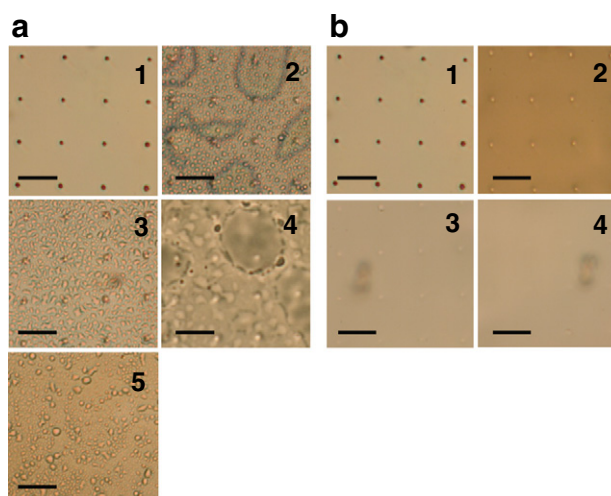
after three days, at which point the polymer was severely degraded. Partially-degraded films were imaged on SEM, and unhealed pores were still clearly visible with only minor morphology changes (Supplementary information). When incubated dry, healing proceeded similar to that of dry-healed ester-terminated PLGA films, but required higher temperatures. For example, the lowest temperature used was 55 °C, which took over 5 days before complete healing was observed (see Fig. 4).

*3.1.4. Fitting Williams–Landel–Ferry (WLF) and Arrhenius equations to PLGA healing data*

In order to test if polymer healing was dependent on the viscoelastic properties of the polymer, as would be expected if healing occurs by material flow to minimize surface energy, the healing times of 5-μm pores in both dry (ester- and acid-terminated polymers) and aqueous (ester-terminated only) conditions were fit by the Williams–Landel–Ferry equation for time–temperature superposition:

$$\text{Log}\left(\frac{t}{t_o}\right) = \frac{-C_1(T-T_o)}{C_2+(T-T_o)} \tag{1}$$

where t and T are time and temperature, respectively; t_o is the reference time at the reference temperature T_o, and C_1 and C_2 are constants. When T_g is used as the reference temperature T_o, then the constants C_1 and C_2 become universal values of 17.4 and 51.6 K, respectively [23]. The T_g recorded during the first heating cycle of MDSC was used (see Table 1), as this best simulates experimental conditions. Data were independently fit using non-linear regression to determine t_o for all data sets. As shown in Fig. 4, the WLF equation could be adequately fit to the data [$r^2 > .951$], yielding $t_o = 1.78 \cdot 10^6$ h, $4.35 \cdot 10^6$ h, and $2.4 \cdot 10^8$ h for lauryl ester-terminated dry and wet films, and acid-end group dry films, respectively.

Table 1
Residual solvent and glass-transition temperature measurements as determined by TGA and MDSC, respectively. The T_g from the first heating cycle was used in further calculations. $n = 3$, $\pm$ SEM.

Polymer end-group	Residual solvent (%)	Raw polymer T_g (°C)		Dried film T_g (°C)		Hydrated film T_g (°C)	
		First heat	Second heat	First heat	Second heat	First heat	Second heat
Lauryl ester	1.7 ± 0.1	42.7 ± 0.3	44.7 ± 0.2	35.4 ± 0.3	40.7 ± 0.3	23.4 ± 0.4	24.0 ± 0.3
Carboxylic acid	3.6 ± 0.4	51.5 ± 0.6	48.4 ± 0.1	26.4 ± 0.4	45.1 ± 1.8	18.7 ± 0.5	18.5 ± 0.6
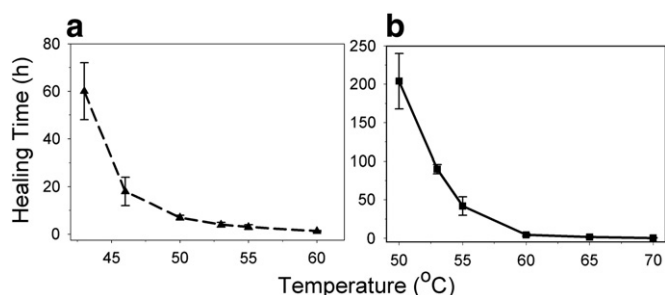
Fig. 3. Effect of temperature on healing time of 5-μm pores on PLGA films incubated in a) PBST and b) air (no hydration). $n = 3$, ± range.

Fig. 5. Healing time as a function of pore width under hydrated conditions at 50 °C. All pores were 7 μm deep. $n = 3$, ± range.
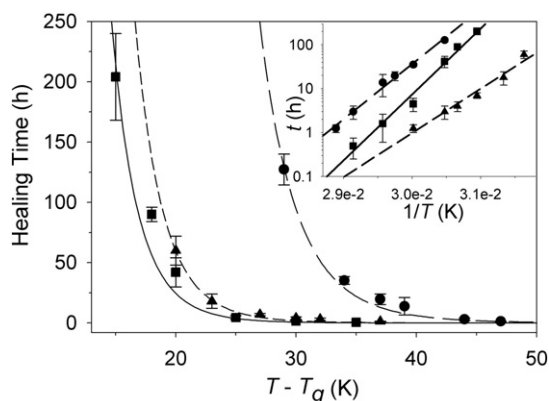
An approximate mechanics analysis of healing indicated that healing times should follow an Arrhenius rate law of the form:
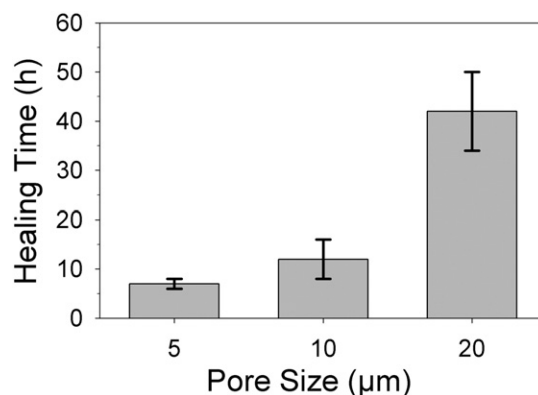
$$t = Ae^{-Q/RT}. \qquad (2)$$

Therefore, to determine the activation energy for the healing process, healing data were individually plotted on an Arrhenius plot ($\ln(t)$ vs. $1/T$) (Fig. 4 inset). The activation energy (Q) was determined by dividing the slope of the line by the gas constant, R. The observed values of Q were 288 kJ/mol ($r^2 = .985$), 193 kJ/mol ($r^2 = .973$), and 240 kJ/mol ($r^2 = .991$) for lauryl ester-terminated dry and wet films, and acid-end group dry films, respectively.

3.2. Effect of pore width

Pores could be made using microneedles of 5, 10, 20, 30, and 50 μm wide, all at a depth of 7 μm. When incubated in PBST, the healing time was found to increase with pore width for the 5, 10, and 20 μm pores (Fig. 5). Pores of 30 and 50-μm size displayed the beginning signs of pore closing (i.e. pores had become circular, and were becoming less distinct − consistent with healing in the smaller pores). However, complete healing was not observed by 48 h, at which time the films were so significantly damaged by degradation that further observations were not possible (Fig. 6a). Had a thicker film or non-degradable polymer been used, it is likely that these pores would have healed eventually.
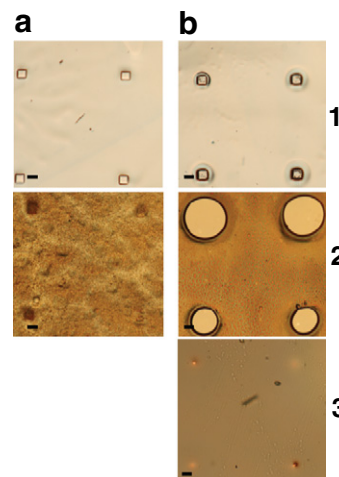
3.3. Effects of pore depth

A set of pores with a depth of 15 μm, which extended them more than halfway through the 26 μm film, were also made with widths of 50, 100, 150, and 250 μm. When incubated in aqueous conditions at 50 °C, these pores tended to rupture rather than heal (Fig. 6b). That is, the pores went from initially being a dent on the film surface, to a through-hole that extended to the glass substrate. The polymer at the bottom of the pores tore away from the glass, and the pores grew up to 300% in diameter while becoming more circular. The larger pores tended to rupture less often than the smaller ones, although none demonstrated healing during the times studied (up to 48 h).

When the study was conducted under dry conditions at 60 °C, the rupturing phenomenon was not typically observed. These pores showed some signs of the onset of healing, but did not heal fully on the relevant time scale (<2 weeks). The pores had clearly become smaller and less distinct, but never fully disappeared. On rare occasions, some of the pores did rupture, but did not grow as they had in the aqueous experiment.

4. Discussion

The model system of using PLGA films stamped with a microneedle array proved to be a reliable system for reproducibly measuring pore-healing. Pores could be made of controlled width and depth,

Fig. 4. WLF describes healing time of 5 μm pores in lauryl ester-terminated PLGA incubated in PBST (▲) or dry (■) conditions, and carboxylic acid-terminated PLGA incubated dry (●). Data from Fig. 3 was fitted by non-linear regression to WLF equation using $T_o = T_g$, $C_1 = 17.4$ K, and $C_2 = 51.6$ K. $r^2 = .951$ (ester-terminated dry), .993 (ester-terminated in PBST), and .981 (acid-terminated dry). Inset: Arrhenius plot of healing data. Resulting activation energies were 288 kJ/mol for dry incubation ($r^2 = .985$), 193 kJ/mol for incubation in PBST ($r^2 = .973$), and 240 kJ/mol for acid-capped PLGA incubated dry ($r^2 = .991$).

Fig. 6. Light micrographs of microneedle-stamped PLGA pores (50 μm wide) after incubation. a) 7 μm deep. b) 15 μm deep. 1) Before incubation. 2) After incubation in PBST. 3) After incubation in air. Scale = 50 μm.

and could be individually monitored by light microscopy or occasionally SEM. This method did demonstrate difficulties creating pores smaller than 5 μm, which may have been because the polymer solution was able to relax back into these small pores, or because the 10× inter-needle distance was not sufficient in these instances. An alternative currently being explored for making smaller surface pores is physical indentation by the tip of an Atomic Force Microscope (AFM), similar to a previously reported study [24]. In addition, Axelsson et al. used ZnCl₂ as a pore forming excipient in PLGA films, but this method produced pores with great polydispersity and it was not possible to have precise control over the number or spacing of the pores [25].

After drying, the films contained a slightly elevated level of residual solvent, but this was expected since drying at elevated temperature (annealing) could not be done, as it would also begin to heal the pores. The glass-transition temperatures recorded are in reasonable agreement with previously reported values, and a drop in T_g for the hydrated films is consistent with the plasticization effect of water on the polymer [15]. The change in T_g in the dry films compared to the raw polymer is likely due to residual solvent, which is partially released during the first heating cycle, and leads to the higher T_g seen on the second heating cycle. Since the acid-terminated films had more residual solvent, the T_g increases more dramatically between cycles. While the first T_g was used for analysis, the true T_g likely changes slightly during the course of the experiment as more solvent evaporates or more water enters the polymer matrix [25].

It is known that mid-to-high Mw PLGA films have a high interfacial tension, particularly in aqueous environments. This is frequently demonstrated by low wettability and/or a high water droplet contact angle, and is the result of a combination of van der Waals interactions, hydrophobic interactions, and preference of the methyl side chains of lactic acid units to orientate to the polymer/air interface [25–28]. While lauryl ester-terminated PLGAs are particularly hydrophobic, carboxylic acid-terminated PLGAs are less so. This results in weaker hydrophobic interactions, and lower surface stresses as evident by more acute water-droplet contact angles [29]. While these effects are particularly pronounced in aqueous environments, they also affect dry healing under ambient humidity, and weaken the tension at the polymer–air interface.

The results presented here are consistent with a model for pore healing driven by surface tension and controlled by the rate of deformation of the polymer. In the absence of any other stresses, the surface tension and local curvature set up a stress field that drives flow of the polymer to reduce the surface area and, hence, heal the pores. A simple special case that serves to illustrate the physics of the phenomenon is the healing of a spherical pore in a linear viscous material. The von Mises effective stress ($\tilde{\sigma}$) at a distance r from the surface of the sphere is given by

$$\tilde{\sigma} = 3\gamma a^2 / r^3 \tag{3}$$

where γ is the surface tension of the material, and a is the radius of the pore. Assuming that the material obeys a Levy–Mises flow rule with a linear relationship between the effective stress and effective strain rate ($\dot{\tilde{\varepsilon}}$):

$$\dot{\tilde{\varepsilon}} = \tilde{\sigma} / 3\eta \tag{4}$$

where η is the viscosity. Assuming a single thermally-activated mechanism for flow, with an activation energy Q, the viscosity is of the form

$$\eta = \eta_o \exp(Q/RT) \tag{5}$$

where η_o is a material constant, R is the molar gas constant, and T is the absolute temperature. These equations can be used to show that the healing time (t) for a spherical pore is given by

$$t = 2\eta_o a_o \exp(Q/RT)/\gamma \tag{6}$$

where a_o is the initial pore radius.

While this model has an oversimplified geometry and, probably, an oversimplified constitutive law, it does provide a good connection to many of the experimental observations. Firstly, it should be noted that the transition from the square pore to the rounded shape is a classic sign of a surface-tension driven phenomenon. The stresses that drive flow are inversely dependent on the local radius of curvature (as in Eq. (3)), so there is a very large driving force for the sharp corners of a square to be rounded out, and the pore to take up a circular shape to minimize surface energy. Secondly, Eq. (6) shows that the healing time is proportional to the initial pore size. A linear relationship would be a direct consequence of a linear constitutive law; non-linear materials would exhibit a non-linearity in this relationship. While there are only three data points in Fig. 5, the data are in general agreement with what would be expected in this type of phenomenon. In ester-terminated PLGA, it is noted that all the pores 7 μm in depth began to heal when incubated above T_g in aqueous conditions, but not all pores managed to close completely before significant degradation took place. The potential of an upper size limit on healing has great implications for PLGA devices used in controlled release; since the healing phenomenon is now gaining interest as a possible encapsulation strategy [13], it suggests that particularly large pores may not heal before a degradation phase begins. Any unhealed pores would contribute significantly to burst release upon incubation in release media. This may limit or add additional considerations to the types of PLGA devices that are considered for paradigm. Lastly, Eq. (6) suggests that an Arrhenius plot will give the activation energy for the flow process. Fig. 4 shows such a plot, indicating activation energies of roughly 288 kJ/mol and 193 kJ/mol for the ester-terminated polymer in dry and wet conditions, respectively, and 240 kJ/mol for dry acid-terminated PLGA — values within the somewhat wide range of apparent activation energies reported for polymer flow and relaxation [30–32]. A lower activation energy for the hydrated polymer is expected, as water acts as a lubricant to polymer flow. Also, despite healing slower, a lower activation energy for acid-terminated PLGA compared to the ester-terminated PLGA is expected. The former has a lower Mw and a further depressed T_g, so the polymer chains have more freedom to move, and can do so more readily. However, the observed healing kinetics are slower in acid-terminated PLGA due to a lower overall driving force. This is an important distinction with regard to self-healing in PLGA microspheres, as choosing a more mobile polymer may not always promote faster self-healing unless the effect on other parameters, notably surface tension, is considered as well.

Data from Figs. 2 and 3, along with the T_g information, indicate that healing of the microneedle-stamped pores takes place in a reasonable time-frame when the polymer is in the rubbery state above the T_g, but not in the glassy state below it. The temperature–time shift associated with the WLF equation for polymers is another manifestation of a thermally-activated process, with significant mobility being associated with temperatures above the glass-transition temperature. Driven by the stress of surface tension, this enhanced mobility allows viscoelastic flow of the polymer to heal the defect. This flow in response to surface tension could be considered a form of creep that occurs when $T > T_g$. Although healing was not observed in aqueous conditions at 37 °C, it is clear from previous research that healing at this temperature is possible [13]. The WLF equation predicts that pores would have healed if experiments were carried out longer (35 days for healing in PBST at 37 °C, 65 days for dry healing at 46 °C). Microspheres typically have smaller pores, and may have greater surface tension caused by a very different manufacturing process, or a lower T_g due to the inclusion of excipients, thus allowing them to heal faster at 37 °C than is predicted here. Additionally, the reason pores in PLGA 504H did not heal when exposed to aqueous conditions is likely two-fold. First, this polymer degrades much faster than ester-capped PLGA, limiting the window over which healing can be easily measured. Second, the lower hydrophobicity caused by the presence of the carboxylic acid severely weakens the surface tension driving force.

The behavior of 15-μm deep pores when incubated under aqueous conditions was particularly intriguing. These pores did not heal, and in fact grew in size significantly and caused damage to the film. It is possible that this occurred because the films were spin-coated to a glass substrate, and this allowed an in-plane stress to develop, as has been previously reported [33]. Therefore, the rupturing phenomenon might not be expected to extend to free-standing PLGA microspheres. Nonetheless, whether a pore will heal or extend and rupture depends on a competition between elastic strain energy and surface energy. The relative importance of these two terms is measured by the dimensionless group $\sigma a_o/\gamma E$ [34], where E is the appropriate elastic modulus of the polymer, and σ is the normal stress at the tip of the pore. If the value of this group is small, the problem is dominated by surface tension, and the pore is expected to heal. Conversely, if the value of this group is large, the problem is dominated by the elastic energy term and rupture is favored. It is possible that rupturing occurred more commonly under wet conditions because of moisture uptake by the polymer leading to an enhanced stress. It should be noted that swelling caused by moisture uptake for microparticles and other PLGA devices might cause the pores to open initially [7], depending on the relative time scales for moisture absorption and healing. Whether the pores would eventually heal or not would likely depend on the nature of any geometrical constraint (similar as that provided by the glass substrate) that might result in the evolution of elastic stresses.

5. Conclusion

Healing of PLGA devices is an important phenomenon with strong implications for affecting release kinetics and providing an avenue for aqueous-based encapsulation of large molecules. The microneedle-stamped films used here are a simple way to study this phenomenon in a controlled pore geometry. This system allowed the healing behavior of different PLGAs exposed to various conditions to be identified, and the data was adequately described by universal WLF and Arrhenius behavior. Self-healing was consistent with a surface tension driven process, causing creep when the polymer was above the T_g and chain motion via viscoelastic flow was possible. In the future, this approach may allow more quantitative assessment of healing in PLGA and other biomaterials.

Supplementary data to this article can be found online at http://dx.doi.org/10.1016/j.jconrel.2013.06.035.

References

[1] D.H. Lewis, Controlled release of bioactive agents from lactide/glycolide polymers, in: M. Chasin, R. Langer (Eds.), Biodegradable Polymers as Drug Delivery Systems, Marcel Dekker, New York, 1990, pp. 1–41.
[2] L.J. Cleland, A.J. Jone, Stable formulation of recombinant human growth hormone and interferon-gamma for microencapsulation in biodegradable microspheres, Pharm. Res. 13 (1996) 1464–1475.
[3] S.P. Schwendeman, H.R. Costantino, R.K. Gupta, M. Tobio, A.C. Chang, M.J. Alonso, G.R. Siber, R. Langer, Strategies for stabilizing tetanus toxoid toward the development of a single-dose tetanus vaccine, Dev. Biol. Stand. 87 (1996) 293–306.
[4] K.A. Woodrow, C.J. Booth, J.K. Saucier-Sawyer, M.J. Wood, W.M. Saltzman, Intravaginal gene silencing using biodegradable polymer nanoparticles densely loaded with small-interfering RNA, Nat. Mater. 8 (2009) 526–533.
[5] K.G.H. Desai, S.R. Mallery, A.S. Holpuch, S.P. Schwendeman, Development and in vitro-in vivo evaluation of fenretinide-loaded oral mucoadhesive patches for site-specific chemoprevention of oral cancer, Pharm. Res. 28 (2011) 2599–2609.
[6] S.S. Venkatraman, L.P. Tan, J.F.D. Joso, F. Boey, X.T. Wang, Biodegradable stents with elastic memory, Biomaterials 27 (2006) 1573–1578.
[7] J. Wang, B. Wang, S.P. Schwendeman, Characterization of the initial burst release of a model peptide from poly(D,L-lactide-co-glycolide) microspheres, J. Control. Release 82 (2002) 289–307.
[8] S.P. Schwendeman, J. Kang, S. Reinhold, Methods for encapsulation of biomacromolecules in polymers, US Patent No. 8017155B2 (2011).
[9] S. Reinhold, Self-healing Polymers Microencapsulate Biomacromolecules Without Organic Solvents. Ph.D. Thesis University of Michigan, 2009.
[10] G. Zhu, S.R. Mallery, S.P. Schwendeman, Stabilization of proteins encapsulated in injectable poly(lactide-co-glycolide), Nat. Biotechnol. 18 (2000) 52–57.
[11] C. Pérez, G. Kai, Effects of salt on lysozyme stability at the water–oil interface and upon encapsulation in poly(lactic-co-glycolic) acid microspheres, Biotechnol. Bioeng. 82 (2003) 825–832.
[12] S.P. Schwendeman, M. Cardamone, M. Brandon, A. Klibanov, R. Langer, Stability of proteins and their delivery from biodegradable polymer microspheres, in: S. Cohen, H. Bernstein (Eds.), Microparticulate Systems for the Delivery of Proteins and Vaccines, Marcel Dekker, New York, 1996, pp. 1–50.
[13] S.E. Reinhold, K.G.H. Desai, L. Zhang, K.F. Olsen, S.P. Schwendeman, Self-healing microencapsulation of biomacromolecules without organic solvents, Angew. Chem. Int. Ed. 51 (2012) 10800–10803.
[14] J. Kang, S.P. Schwendeman, Pore closing and opening in biodegradable polymers and their effect on the controlled release of proteins, Mol. Pharm. 4 (2007) 104–118.
[15] P. Blasi, S.S. D'Souza, F. Selmin, P.P. DeLuca, Plasticizing effect of water on poly(lactide-co-glycolide), J. Control. Release 108 (2005) 1–9.
[16] H. Sah, Protein behavior at the water/methylene chloride interface, J. Pharm. Sci. 8812 (1999) 1320–1325.
[17] Y.F. Maa, C.C. Hsu, Protein denaturation by combined effect of shear and air–liquid interface, Biotechnol. Bioeng. 54 (1997) 503–512.
[18] S.J. Prestrelski, N. Tedeschi, T. Arakawa, J.F. Carpenter, Dehydration-induced conformational transitions in proteins and their inhibition by stabilizers, Biophys. J. 65 (1993) 661–671.
[19] W.R. Lie, R. Langer, A.M. Klibanov, Moisture-induced aggregation of lyophilized proteins in the solid-state, Biotechnol. Bioeng. 37 (1991) 177–184.
[20] C.E. Holy, C. Cheng, J.E. Davies, M.S. Shoichet, Optimizing the sterilization of PLGA scaffolds for use in tissue engineering, Biomaterials 22 (2001) 25–31.
[21] P. Alexander, L.D.G. Hamilton, A. Stacey, Irradiation of proteins in the solid state: I. Aggregation and disorganization of secondary structure of bovine serum albumin, Radiat. Res. 12 (1960) 510–525.
[22] S. Kim, D. Hong, Y. Chung, H. Sah, Ammonolysis-induced solvent removal: a facile approach for solidifying emulsion droplets into PLGA microspheres, Biomacromolecules 8 (2007) 3900–3907.
[23] S.P. Zaoutsos, G.C. Papanicolaou, Viscoelastic constitutive modeling of creep and stress relaxation in polymer and polymer matrix composites, in: R.M. Guedes (Ed.), Creep and Fatigue in Polymer Matrix Composites, Woodhead Publishing in Materials, Pennsylvania, 2011, pp. 1–45.
[24] J.A. Yoon, J. Kamada, K. Koynov, J. Mohin, T. Kowalewski, K. Matyjaszewski, Self-healing polymer films based on thiol–disulfide exchange reaction and self-healing kinetics measured using atomic force microscopy, Macromolecules 45 (2012) 142–149.
[25] S. Fredenberg, M. Wahlgren, M. Reslow, A. Axelsson, Pore formation and pore closure in poly(D,L-lactide-co-glycolide) films, J. Control. Release 150 (2011) 142–149.
[26] E.I. Vargha-Butler, E. Kiss, C.N. Lam, Z. Keresztes, E. Kalman, L. Zhang, A.W. Neumann, Wettability of biodegradable surfaces, Colloid Polym. Sci. 279 (2001) 1160–1168.
[27] N.B. Viswanathan, S.S. Patil, J.K. Pandit, A.K. Lele, M.G. Kulkarni, R.A. Mashelkar, Morphological changes in degrading PLGA and P(DL)LA microspheres: implications for the design of controlled release systems, J. Microencapsul. 18 (2001) 783–800.
[28] T.G. Park, Degradation of poly(D,L-lactic acid) microspheres: effect of molecular weight, J. Control. Release 30 (1994) 61–173.
[29] J.Y. Yoo, S. Mitragotri, Polymer particles that switch shape in response to a stimulus, PNAS 107 (2010) 11205–11210.
[30] Y.M. Boiko, Interdiffusion of polymers with glassy bulk, Colloid Polym. Sci. 289 (2011) 1847–1854.
[31] J.F. Mano, Study of the segmental dynamics in semi-crystalline poly(lactic acid) using mechanical spectroscopies, Macromol. Biosci. 5 (2005) 337–343.
[32] M.L. Williams, R.F. Landel, J.D. Ferry, The temperature dependence of the relaxation mechanisms in amorphous polymers and other glass-forming liquids, JACS 77 (1955) 3701–3707.
[33] P. Damman, G. Sylvain, C. Séverine, S. Despres, D. Villers, G. Reiter, et al., Relaxation of residual stress and reentanglement of polymers in spin-coated films, Phys. Rev. Lett. 99 (2007) 036101-1-4.
[34] Z. Suo, W. Wang, Diffusive void bifurcation in stressed solid, J. Appl. Phy. 76 (1994) 3410–3421.